Single-Macromolecule Fluorescence Resonance Energy Transfer and Free-Energy Profiles

Irina V. Gopich† and Attila Szabo*

Laboratory of Chemical Physics, National Institute of Diabetes and Digestive and Kidney Diseases, National Institutes of Health, Bethesda, Maryland 20892

Received: November 17, 2002; In Final Form: March 5, 2003

What is the dynamical and structural information contained in single-molecule fluorescence resonance energy transfer (FRET) experiments where the donor and acceptor photons emitted during a fixed time window T are counted? To answer this question, a theory is developed to obtain the probability distribution of the energy-transfer efficiency obtained from trajectories of duration T. The efficiency is an explicit function of the distance between a fluorescent donor and acceptor attached to the macromolecule; thus, the efficiency can formally be converted to a distance. The resulting distance probability distribution or, equivalently, the potential of mean force or free-energy profile, however, depends on the size of the observation time window T. Illustrative calculations are presented for a random coil polymer and for a protein that exhibits two-state folding kinetics. It is found that the apparent free-energy profiles look physically reasonable, even for long observation times during which significant fluctuations occur. Such profiles are, however, deceptive unless the observation time is approximately an order of magnitude smaller than the relaxation time of the donor−acceptor distance.

I. Introduction

In this paper, we consider the problem of extracting the underlying free-energy profile from single-molecule resonance energy-transfer studies of protein folding.[1−3] There are two important classes of single-molecule experiments that can, in principle, be used to determine the free-energy profile along a specific coordinate. In atomic force microscopy pulling experiments, a molecule is subjected to a time-dependent force to pull it along some coordinate (see, for example, the work of Carrion-Vazquez et al.[4]). Even though the system is driven away from equilibrium, it has recently been shown[5] how the free-energy profile along the pulling coordinate can be extracted from repeated nonequilibrium pulling experiments. A second class of experiments, considered here, is the use of Förster resonance energy transfer (FRET) to monitor the spontaneous folding and unfolding of molecules in the presence of chemical denaturants.

In such experiments, a macromolecule is specifically labeled with a fluorescent donor and acceptor. A single molecule is chosen at random from an equilibrium ensemble. Its donor is excited by continuous laser illumination, and the number of photons emitted from the donor and acceptor in a fixed time window are counted. The ratio of the number of acceptor photons to the total number of photons is the energy-transfer efficiency, which depends on the distance between the donor and acceptor dyes. This distance fluctuates, not only because the protein can convert between a folded and unfolded state, but also because of conformational dynamics in each of these states. If the observation time window is long enough for a sufficient number of photons to be emitted, so that shot noise is negligible, but short enough so that the donor−acceptor distance does not change, then the efficiency can be converted to a meaningful distance. When this experiment is repeated on many single molecules, the probability distribution of the distance can be determined. The logarithm of this distribution gives the potential of mean force or the free-energy profile along the interdye distance coordinate.

What happens if the donor−acceptor distance changes during the observation time? Clearly, if this time is longer than all relaxation times characterizing the dynamics of the system, each observation would simply give the average efficiency that can be obtained from a bulk experiment. In this paper, we show how to calculate the probability of finding a specific value of the efficiency for arbitrary observation times, given a microscopic model of the dynamics. Our results are applicable to any observable averaged over a finite time interval. The variance and mean of the distribution are well-known in the area of computer simulations in the context of estimating the error in some quantity obtained by averaging over trajectories of finite duration.[6] In the area of single-molecule spectroscopy, the distribution of the populations in a two-state system has been evaluated.[7,8]

The outline of this paper is as follows. In Section II, we discuss the behavior of the probability distribution of an observable averaged over short and long trajectories. In Section III, we present the general formulation and briefly outline our numerical method to calculate the probability distribution for arbitrary observation times. The details are presented in the Appendix. In Section IV, we first apply our formalism to an unfolded protein, where the interdye distance distribution is Gaussian and the dynamics is described as diffusion on the corresponding potential surface. Some of the results obtained here have recently been used by Schuler et al.[3] in extracting a lower bound to the free-energy barrier to protein folding from their single-molecule FRET experiments. We then consider longer observation time windows, where transitions between folded and unfolded states can occur. We find that the apparent free-energy profiles can look physically reasonable, even when

* Author to whom correspondence should be addressed. E-mail: attilas@nih.gov.

† On leave from the Institute of Chemical Kinetics and Combustion SB RAS, Novosibirsk, 630090, Russia.

10.1021/jp027481o
Published on Web 04/30/2003

the observation time is so long that the experiment contains only limited information about the actual shape of the profiles.

II. Theory

A. Some Limiting Results. Consider a molecule chosen at random from an equilibrium ensemble and monitored for time T. In this time window, the average value of a property $a(r)$ that depends on a fluctuating coordinate $r(t)$ is

$$\bar{a} = \frac{1}{T}\int_0^T a(r(t))\,\mathrm{d}t \tag{2.1}$$

Each measurement results in a different value of $\bar{a}$, and we are interested in the probability distribution of $\bar{a}$ for a given observation time T, $p(\bar{a}|T)$. In this paper, we show how to obtain this probability distribution, given a microscopic model of the dynamics without generating long trajectories via computer simulations. Although our formalism is rather general, we are specifically interested in the special case $a(r) = E(r)$, where $E(r)$ is the efficiency of Förster energy transfer between a fluorescent donor and an acceptor separated by a distance r and $E(r) = (1 + (r/R_0)^6)^{-1}$ (where R_0 is the Förster radius, i.e., the distance at which the efficiency is $^1/_2$). This expression is valid when angular averaging of the dipole−dipole interaction occurs, because of fast local motions of the fluorophores. The distance r then fluctuates because of the dynamics of the macromolecule to which the fluorescent probes are attached.

For very short observation times ($T \to 0$),

$$p(\bar{a}|0) = \int f_{\mathrm{eq}}(r)\delta(\bar{a} - a(r))\,\mathrm{d}r = \left[\frac{f_{\mathrm{eq}}(r)}{\left|\frac{\mathrm{d}a(r)}{\mathrm{d}r}\right|}\right]_{r^*} \tag{2.2}$$

where $f_{\mathrm{eq}}(r)$ is the underlying equilibrium probability distribution and $r^* = a^{-1}(\bar{a})$ is the solution of $a(r) = \bar{a}$. Thus, for short observation times, one can reconstruct the equilibrium distribution of r from the measurement of the distribution of $\bar{a}$:

$$f_{\mathrm{eq}}(r) = \frac{\exp(-\beta V(r))}{\int \mathrm{d}r\,\exp(-\beta V(r))} = p(a(r)|0)\left|\frac{\mathrm{d}a(r)}{\mathrm{d}r}\right| \tag{2.3}$$

where $1/\beta = k_{\mathrm{B}}T$. One can formally use this relation for arbitrary observation times and thus define (to within a constant) an apparent potential of mean force that is dependent on the size of the time window:

$$\beta V_{\mathrm{app}}(r|T) = -\ln\left(p(a(r)|T)\left|\frac{\mathrm{d}a(r)}{\mathrm{d}r}\right|\right) \tag{2.4}$$

Only in the limit $T \to 0$ does V_{app} approach the true free-energy profile.

When $T \to \infty$,

$$p(\bar{a}|\infty) = \delta(\bar{a} - \langle a\rangle) \tag{2.5}$$

where $\langle a\rangle = \int a(r) f_{\mathrm{eq}}(r)\,\mathrm{d}r$ is the equilibrium average of a, which can be obtained from ensemble measurements.

The mean of the distribution $p(\bar{a}|T)$ is $\langle a\rangle$ for all T values; however, its variance depends on T:

$$\sigma^2(T) \equiv \langle \bar{a}^2\rangle - \langle a\rangle^2 = \frac{2}{T^2}\int_0^T (T - t)\langle \delta a(t)\delta a(0)\rangle\,\mathrm{d}t \tag{2.6}$$

where $\delta a(t) = a(r(t)) - \langle a\rangle$. As $T \to \infty$, this becomes

$$\sigma^2(T) \approx \frac{2}{T}\int_0^\infty \langle \delta a(t)\delta a(0)\rangle\,\mathrm{d}t = \frac{2\tau_a}{T}(\langle a^2\rangle - \langle a\rangle^2) \tag{2.7}$$

where τ_a is the relaxation time of the autocorrelation function of $a(r(t))$, defined as $\tau_a = \int_0^\infty \langle \delta a(t)\delta a(0)\rangle/\langle \delta a^2\rangle\,\mathrm{d}t$. If the autocorrelation function does not decay faster than $1/t$, the variance is infinite and eq 2.9 (given below) is not valid. These results are well-known in the area of computer simulations,[6] where they can be used to estimate the error in an average obtained from trajectories of finite duration. If the correlation function describing the fluctuations of $a(r(t))$ can be approximated by a single exponential, $\langle \delta a(t)\delta a(0)\rangle/\langle \delta a^2\rangle = \exp(-t/\tau_a)$, then $\sigma^2(T)$ becomes

$$\sigma^2(T) = \frac{2\tau_a}{T}(1 - \tau_a(1 - \mathrm{e}^{-T/\tau_a})/T)(\langle a^2\rangle - \langle a\rangle^2) \tag{2.8}$$

At long times T, it follows from the central limit theorem that the distribution of $\bar{a}$ is a Gaussian:

$$\lim_{T\to\infty} p(\bar{a}|T) = (2\pi\sigma^2(T))^{-1/2}\exp\left(-\frac{(\bar{a} - \langle a\rangle)^2}{2\sigma^2(T)}\right) \tag{2.9}$$

It is interesting to note that this Gaussian approximation with $\sigma^2(T)$, given in eq 2.8, turns out to be exact for all times for the following problem. A Brownian particle diffuses in a harmonic potential $\beta V(x) = x^2/(2\langle x^2\rangle)$ with diffusion constant D (i.e., the Ornstein−Uhlenbeck process[9]). The distribution of the average value of its position ($a(t) = x(t)$) calculated from trajectories of length T then is given by eqs 2.9 and 2.8, with $a = x$ and $\tau_a = \langle x^2\rangle/D$ for all T values. For diffusion in an arbitrary, one-dimensional potential, the value of $\sigma^2(T)$ cannot be found analytically. However, its long-time limit can be shown to be

$$\sigma^2(T) \approx \frac{2}{DT}\int_{x_{\mathrm{m}}}^{x_{\mathrm{M}}} \frac{\mathrm{d}x}{f_{\mathrm{eq}}(x)}\left[\int_{x_{\mathrm{m}}}^{x} \delta a(y) f_{\mathrm{eq}}(y)\,\mathrm{d}y\right]^2 \tag{2.10}$$

where x_{m} and x_{M} are the minimum and maximum values of x, respectively, and $f_{\mathrm{eq}}(x)$ is the normalized equilibrium distribution ($f_{\mathrm{eq}}(x) = \exp(-\beta V(x))/\int_{x_{\mathrm{m}}}^{x_{\mathrm{M}}} \exp(-\beta V(x))\,\mathrm{d}x$).

These results in the contest of energy-transfer efficiency measurements show that, for sufficiently long observation times, when eq 2.7 becomes valid, the variance of the efficiency distribution contains only limited information. Specifically, one can only determine the product of the relaxation time and the equilibrium variance of the efficiency. To estimate these separately, measurements at observation times comparable to the efficiency relaxation time are required (see eq 2.8).

B. General Formalism. We now consider how $p(\bar{a}|T)$ can be obtained numerically for arbitrary observation time windows T. This distribution can be written as

$$p(\bar{a}|T) = \left\langle \delta\left(\bar{a} - \frac{1}{T}\int_0^T a(r(t))\,\mathrm{d}t\right)\right\rangle = \frac{T}{2\pi}\int_{-\infty}^{\infty} \mathrm{e}^{iw\bar{\alpha}} q(w|T)\,\mathrm{d}w \tag{2.11}$$

where we have used the Fourier representation of the δ-function and defined $\bar{\alpha} = \bar{a}T$ and

$$q(w|T) = \langle \exp(-iw\int_0^T a(r(t))\,\mathrm{d}t)\rangle \tag{2.12}$$

For Markovian dynamics, from Kubo-Anderson line shape theory[10−12] or the Feinman-Kac theorem,[13] it follows that $q(w|T) = \int f(r,T;\, w)\, \mathrm{d}r$, where

$$\frac{\partial}{\partial t} f(r,t;\, w) = \mathscr{L} f(r,t;\, w) - iwa(r) f(r,t;\, w) \qquad (2.13)$$

with the initial condition $f(r,0;\, w) = f_{\mathrm{eq}}(r)$. $\mathscr{L}$ is the operator that describes the dynamics, and $\mathscr{L} f_{\mathrm{eq}}(r) = 0$. Solving this equation and inverting the Fourier transform yields the desired distribution. This can be done analytically only in few special cases. For the sake of notational simplicity, we have assumed that the dynamics along the (one-dimensional) coordinate r is Markovian. This formalism can be immediately generalized to higher-dimensional Markovian processes and, consequently, to non-Markovian dynamics along r.

The short- and long-time T behavior of $p(\bar{a}|T)$ are given by eqs 2.2 and 2.9. It is possible to construct an approximation for $p(\bar{a}|T)$ that is exact in both short and long times. For the illustrative examples considered in this paper, this expression does not work very well at intermediate times; however, it may be useful in other contexts. Therefore, for the sake of completeness, we quote it here:

$$p(\bar{a}|T) = \int \mathrm{d}r_0 \, \frac{f_{\mathrm{eq}}(r_0)}{\sqrt{2\pi\sigma^2(T|r_0)}} \exp\left(- \frac{(\bar{a} - \langle \bar{a}(T|r_0)\rangle)^2}{2\sigma^2(T|r_0)} \right) \qquad (2.14)$$

where $\langle \bar{a}(T|r_0)\rangle$ is the average value of $\bar{a}$ at time T, given that the system was initially at r_0:

$$\langle \bar{a}(T|r_0)\rangle = \frac{1}{T}\int_0^T \mathrm{d}t \int \mathrm{d}r \; a(r) G(r,t|r_0,0) \qquad (2.15)$$

and

$$\sigma^2(T|r_0) = \frac{1}{T^2}\int_0^T \mathrm{d}t \int_0^T \mathrm{d}t' \int \mathrm{d}r \, \mathrm{d}r' \; a(r) G(r,t|r',t') a(r') G(r',t'|r_0,0) - \langle \bar{a}(T|r_0)\rangle^2 \qquad (2.16)$$

Here, $G(r,t|r',t')$ is the Green's function or propagator corresponding to the operator $\mathscr{L}$. It is the probability of finding the system at r at time t, given that it was at r' at time t'.

In general, eq 2.13 must be solved numerically. We have developed an efficient algorithm for doing this. If the operator $\mathscr{L}$ is discretized to obtain an $N \times N$ matrix $\boldsymbol{L}$, it is straightforward to show that the Laplace transform of $q(w|T)$ is given by

$$\hat{q}(w|s) = \boldsymbol{e}^{\mathrm{T}} (s\boldsymbol{I} - \boldsymbol{L} + iw\boldsymbol{A})^{-1} \boldsymbol{f}_{\mathrm{eq}} \qquad (2.17)$$

where $\boldsymbol{e}$ is the vector with unit elements, $\boldsymbol{f}_{\mathrm{eq}}$ is the vector of the discretized equilibrium probabilities, $\boldsymbol{I}$ is the unit matrix, and $A_{ij} = \delta_{ij} a_i$. In the Appendix, we show how, by finding the eigenvalues and eigenfunctions of an appropriate matrix, one can analytically invert the Fourier transform. The Laplace transform is then inverted numerically, using the Stehfest algorithm.[14]

The simplest example of this formalism is when the system jumps between two states:

$$1 \underset{k_2}{\overset{k_1}{\leftrightarrow}} 2$$

The quantity of interest has value a_i in state i. The probability distribution for $p(\bar{a}|T)$ has been found analytically[8] for the special case $a_i = \delta_{i1}$ (i.e., the population in state 1 is monitored). The more general result can be obtained from this special case, using a simple transformation. The result is (for $a_1 > a_2$)

$$p(\bar{a}|T) = (a_1 - a_2)^{-1} \exp(-kzT)[f_{\mathrm{eq}}^{(1)}\delta(1-x) + f_{\mathrm{eq}}^{(2)}\delta(x) + 2kT f_{\mathrm{eq}}^{(1)} f_{\mathrm{eq}}^{(2)} (I_0(y) + k(1-z)TI_1(y)/y)] \qquad (2.18)$$

where $x = (\bar{a} - a_2)/(a_1 - a_2)$, $k = k_1 + k_2$, $f_{\mathrm{eq}}^{(1)} = k_2/k$, $y = 2kT\sqrt{f_{\mathrm{eq}}^{(1)} f_{\mathrm{eq}}^{(2)} x(1-x)}$, $z = f_{\mathrm{eq}}^{(1)}(1-x) + f_{\mathrm{eq}}^{(2)} x$, and $I_n(y)$ are modified Bessel functions of the first kind.

III. Illustrative Examples

A. Random Coil Polymer. We now consider the distribution of the efficiency of energy transfer between two fluorophores attached to the ends of an unfolded protein modeled as a Gaussian chain. The normalized ($\int_0^\infty f_{\mathrm{eq}}(r)\, \mathrm{d}r = 1$) end-to-end distance distribution is $f_{\mathrm{eq}}(r) = (2\pi\langle r^2\rangle/3)^{-3/2} 4\pi r^2 \exp(-3r^2/(2\langle r^2\rangle))$. The dynamics is described as diffusion on potential $\beta V(r) = -\ln(f_{\mathrm{eq}}(r))$.[15] For this model, the end-to-end distance correlation function is $\langle \boldsymbol{r}(t)\boldsymbol{r}(0)\rangle/\langle r^2\rangle = \exp(-t/\tau_{\mathrm{r}})$, with relaxation time $\tau_{\mathrm{r}} = \langle r^2\rangle/(3D)$.

We are interested in the probability distribution, $p(\bar{E}|T)$, of the efficiency $E(r) = 1/[1 + (r/R_0)^6]$ for observation time T. At short times, the distribution is

$$p(\bar{E}|0) = \frac{\exp\left(-\left(\frac{3R_0^2}{2\langle r^2\rangle}\right)\left(\frac{1-\bar{E}}{\bar{E}}\right)^{1/3} \right)}{\sqrt{2\pi\bar{E}^3(1-\bar{E})\langle r^2\rangle^3/(3R_0^6)}} \qquad (3.1)$$

At long observation times, ($p(\bar{E}|T)$) becomes Gaussian (see eq 2.9), centered on $\langle E\rangle = \int_0^\infty E(r) f_{\mathrm{eq}}(r)\, \mathrm{d}r$ and with a width given by eq 2.10, with $x_{\mathrm{m}} = 0$ and $x_{\mathrm{M}} = \infty$.

The probability distribution $p(\bar{E}|T)$ can be converted to the apparent potential of mean force or free-energy profile as defined in eq 2.4 with $a(r) = E(r)$. When $T \to 0$, V_{app} approaches the true potential of mean force, $\beta V_{\mathrm{app}}(r,0) = 3r^2/(2\langle r^2\rangle) - 2\ln r + \text{constant}$. However, for long times, it becomes (to within a constant)

$$\lim_{T\to\infty} \beta V_{\mathrm{app}}(r,T) = \frac{T}{4\tau_E}\left(\frac{(E(r) - \langle E\rangle)^2}{\langle E^2\rangle - \langle E\rangle^2} \right) - \frac{1}{2}\ln\left[\frac{9TE^2(r)(1-E(r))^2}{\pi r^2 \tau_E(\langle E^2\rangle - \langle E\rangle^2)} \right] \qquad (3.2)$$

To calculate what happens between the short and long times, we solve eq 2.13 specialized to this problem ($\mathscr{L} f = D(\partial/\partial r) f_{\mathrm{eq}}(r) (\partial/\partial r) f/f_{\mathrm{eq}}(r)$). Using the numerical procedure discussed in the Appendix, $p(\bar{E}|T)$ and $\beta V_{\mathrm{app}}(\bar{E}|T)$ are calculated for $\langle r^2\rangle = R_0^2$ and shown in Figure 1. It can be seen how the equilibrium efficiency distribution, eq 3.1, is transformed to a Gaussian centered at $\langle E\rangle$ as the observation time increases. The times are given in units of the relaxation time for the end-to-end distance τ_{r}. The relaxation time that describes the fluctuations of the efficiency (i.e., $\tau_E = \int_0^\infty \langle \delta E(t)\delta E(0)\rangle/\langle \delta E^2\rangle\, \mathrm{d}t$) is $\tau_E \approx 0.45\tau_{\mathrm{r}}$. The variance is $\langle E^2\rangle - \langle E\rangle^2 \approx 0.11$. From eq 2.7, it follows that $\sigma^2 \approx 0.1\tau_{\mathrm{r}}/T$. This relation was recently used by Schuler et al.[3] to estimate an upper limit to τ_{r} from their FRET measurements of single denatured proteins. They identified T with the average residence time of a freely diffusing molecule in the illuminated volume of their confocal microscope.

In the inset of Figure 1, we present the apparent free-energy profile. The $T = 0$ curve is the true profile. The apparent

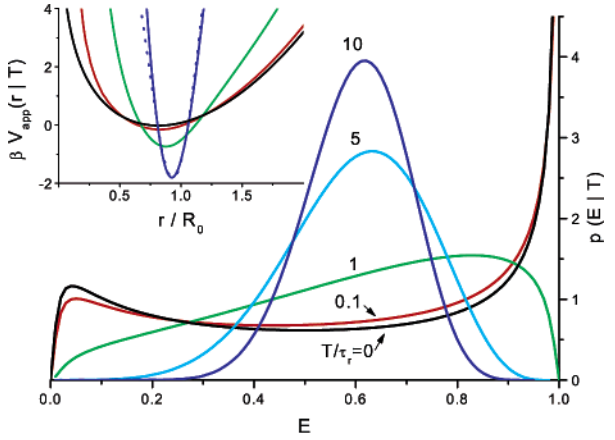

Figure 1. Energy-transfer efficiency distribution $p(\bar{E}|T)$ for the Gaussian chain for different observation times $T/\tau_r = 0$ (black), 0.1 (red), 1 (green), 5 (cyan), and 10 (blue); $R_0^2 = \langle r^2 \rangle$. The diffusion operator was discretized on the grid $r_i = 0.05i$ ($i = 1, ..., 100$), and $J = 8$ was used in eq A9. Inset shows the apparent free-energy profiles $\beta V_{app}(r|T)$; in the inset, the dashed line represents the Gaussian approximation (eq 2.9) for $T/\tau_r = 10$.

potential narrows as the observation time increases. It can be seen that short observation times ($T \approx \tau_r/10$) are needed to determine the potential of mean force accurately. The Gaussian approximation becomes valid when $T \approx 10\tau_r$. It is represented by the dashed line in the inset of Figure 1. Thus, for observation times of $T > 10\tau_r$, the width of the distribution is determined by the combination $\tau_E(\langle E^2 \rangle - \langle E \rangle^2)$, so the relaxation time of the efficiency fluctuations cannot be determined unless one adopts a one-parameter model for the potential that reproduces $\langle E \rangle$ and allows one to calculate $\langle E^2 \rangle$.

B. Two-State Protein Folding. A major objective of single-molecule folding experiments is to determine the free-energy profile along a reaction coordinate.[3] In principle, energy-transfer studies of many single molecules chosen from an equilibrium ensemble can determine the free energy as a function of the donor−acceptor distance if the molecules were rigid during the observation time window. Here, we show that great care must be exercised in analyzing such measurements, because the apparent free-energy profiles can look deceptively reasonable physically, even when significant fluctuations occur.

Consider a two-state protein that can be described by the kinetic scheme

$$F \underset{k_F}{\overset{k_U}{\rightleftarrows}} U$$

Let us suppose that the free-energy surface of this system projected onto a global order parameter such as the fraction of native contacts Q[16] and the donor−acceptor distance r is shown in Figure 2 at the folding temperature where $k_F = k_U$. Similar two-dimensional surfaces are widely used in the protein folding literature.[17,18] In the limit of short observation times, the FRET efficiency can be used to determine the free-energy profile along r, as given by the blue curve in Figure 2. For longer observation times, the apparent free-energy profile along r could be calculated using our numerical procedure, once the nature of the dynamics is specified.

Here, we will consider only observation times that are sufficiently long so that the distribution of the FRET efficiency can be obtained analytically to a good approximation. Consider, first, times that are much longer than the relaxation times of the interdye distance in the folded and unfolded states. In this case, $p(\bar{E}|T)$ would be given by the two-state result in eq 2.18

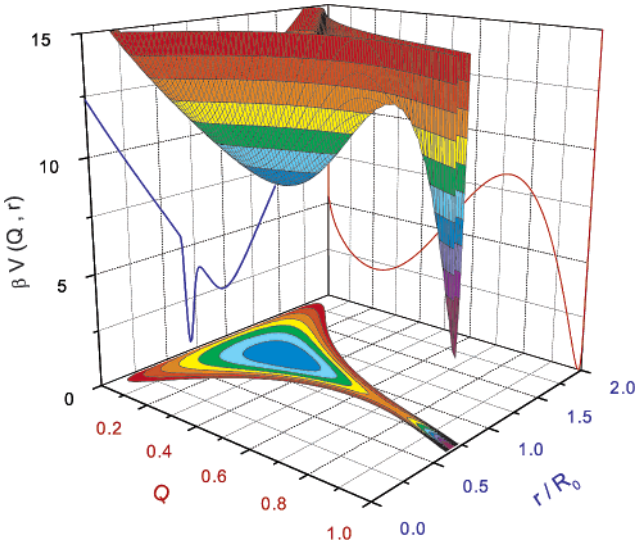

Figure 2. Two-dimensional free-energy surface of a protein as a function of the reaction coordinate Q and the interdye distance r divided by the Förster distance at the folding temperature, where the populations of the folded and the unfolded states are equal. The red curve is the one-dimensional free-energy profile along Q, whereas the blue curve is the free-energy profile along r. The contours are shown at intervals 1 k_BT. The folded state corresponds to high Q and small r. These curves were obtained from the function $\beta V(Q, r) = 100\ Q^3(1 - Q) - 20\ Q/3 - \ln[Q(1 - Q)(1 + Q)^5] + (1 + Q)^{10}[2r/R_0 - 2 + (Q - 0.2)^2]^2 + 8$. The free-energy profile along Q (or r) was obtained by integrating the function $\exp(-\beta V(Q, r))$ over all r (or all Q) values and taking the logarithm. For this potential, $\langle E \rangle_U = 0.52$ and $\langle E \rangle_F = 0.90$, which are the values used in Figure 3.

with $a_1 = \langle E \rangle_F$, $a_2 = \langle E \rangle_U$, and $k = k_F + k_U$, where $\langle E \rangle_F$ and $\langle E \rangle_U$ are the averaged efficiencies in the folded and unfolded states. Let us now generalize this to somewhat shorter observation times, where the distribution function of the efficiency in each of the wells is Gaussian with finite widths.

For sufficiently high barriers, the dynamics within each well is much faster than the transitions between wells and these processes are essentially independent. If we further assume that the width of the $\bar{E}$ distribution in both wells is the same, then $E(t) = E_2(t) + \Delta E_{well}(t)$, where $E_2(t)$ jumps between the averaged efficiencies in each well and $\Delta E_{well}(t)$ describes fluctuations about the averages. Then, $q(w|T)$ in eq 2.12 can be approximated by $\langle \exp(-iw\int_0^T E_2(t)\ dt) \rangle_2 \langle \exp(-iw\int_0^T \Delta E(t)\ dt) \rangle_{well}$. The first term is evaluated using the two-state kinetic model. The second term is approximated by its long-time limit, $\exp(-(wT)^2\sigma^2(T)/2)$, where $T\sigma^2(T) = 2\tau_E^F(\langle E^2 \rangle_F - \langle E \rangle_F^2) = 2\tau_E^U(\langle E^2 \rangle_U - \langle E \rangle_U^2)$ and τ_E^F and τ_E^U are the relaxation times of the efficiency in the folded and unfolded states, respectively. Note that we only assumed that the *product* of the relaxation time and the variance of $\bar{E}$ is the same in these states. This is not unphysical, because both the variance and diffusion coefficient are expected to be smaller in the folded state. Fourier inverting, we obtain the following expression for $p(\bar{E}|T)$, which is valid for times longer than the relaxation times in the folded and unfolded wells:

$$p(\bar{E}|T) = \int_{\langle E \rangle_U}^{\langle E \rangle_F} dE\ p_2(E|T)\ \frac{\exp\left(-\dfrac{(\bar{E} - E)^2}{2\sigma^2(T)}\right)}{\sqrt{2\pi\sigma^2(T)}} \qquad (3.3)$$

where $p_2(\bar{E}|T))$ is given by eq 2.18 with $a_1 = \langle E \rangle_F$, $a_2 = \langle E \rangle_U$, $k_1 = k_F$, $k_2 = k_U$, and $\sigma^2(T) = 2\tau_E(\langle E^2 \rangle - \langle E \rangle^2)/T$.

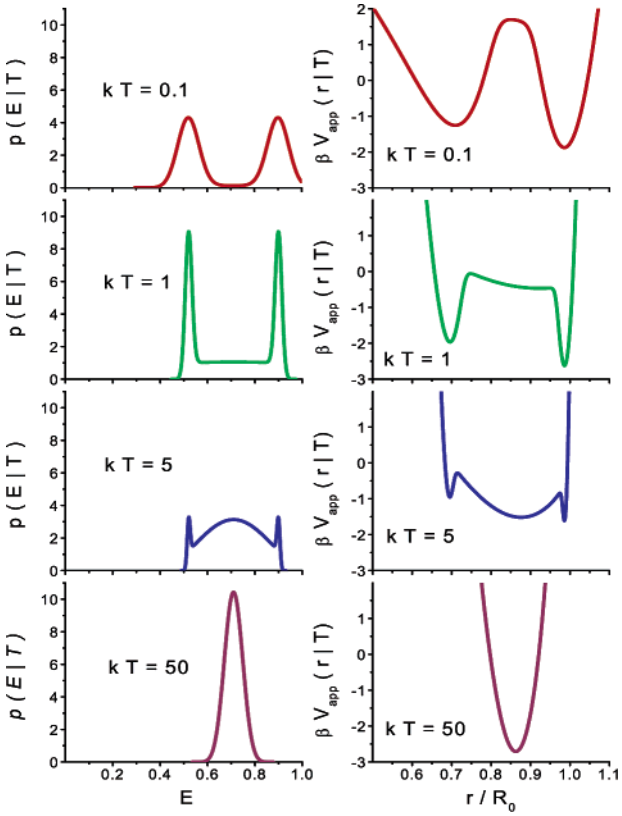

Figure 3. (Left panel) Energy-transfer distribution for a two-state kinetic model of protein folding for times sufficiently long so that the distribution in each of the states is Gaussian. (Right panel) The potential of mean force or corresponding free-energy profiles. The times are in units of $k = k_F + k_U$, $k_F = k_U$, $\langle E\rangle_F = 0.90$, $\langle E\rangle_U = 0.52$, and $\tau_E(\langle E^2\rangle - \langle E\rangle^2) = 10^{-4}$.

Illustrative results are shown in Figure 3 for the free-energy surface in Figure 2, where $\langle E\rangle_F = 0.90$ and $\langle E\rangle_U = 0.52$ and $f_{eq}^F = f_{eq}^U = {}^1/_2$. The times are given in units of $k^{-1} = (k_F + k_U)^{-1}$. The product of relaxation time and variance is assumed to be $\tau_E(\langle E^2\rangle - \langle E\rangle^2) = 10^{-4}$ in both states. Although we do not have to specify the relaxation times in these states, for physically reasonable values of the variance, these times are at least 100 times faster than the folding time. The left panels of Figure 3 shows the change of the efficiency distribution with the observation time T. The right panel presents the corresponding apparent free-energy profiles. At short times, relaxation in the two wells proceeds independently and the distribution is simply a sum of two Gaussians. The widths of these Gaussians narrow as the observation time increases. At $kT = 1$, the exchange between the two wells leads to the appearance of a plateau between two peaks. Comparing the free-energy profiles along r with the true one (the blue curve in Figure 2), it can be seen that only the positions of the minima are correct. The apparent curvatures and barrier heights are artifacts. As T increases, the distribution eventually becomes a Gaussian, centered on the average efficiency of the two states.

The apparent free-energy profiles change dramatically with the observation time and look physically reasonable for a wide range of these times. However, because these were obtained from eq. 3.3, using only the values of the rate constants, the mean values of the efficiency, and the product $\tau_E(\langle E^2\rangle - \langle E\rangle^2)$, they actually contain very limited information about the shape of the true free-energy profile. Thus, one must be cautious in interpreting such profiles extracted from single-molecule experiments of the type considered in this paper. In particular, it is important to establish that the free-energy profiles do not depend on the observation time. If they do, the $p(\bar{E}|T)$ curves can still be used to obtain the folding and unfolding rate constants in a way that is both independent and complementary to the bulk measurements. Moreover, the shapes of the FRET efficiency distributions may be sensitive to the presence of additional thermodynamic states that are difficult to detect in ensemble experiments.

Acknowledgment. We thank Bill Eaton and Sasha Berezhkovskii for helpful discussions.

Appendix A: The Numerical Solution

Discretizing the operator $\mathscr{L}$ leads to a $N \times N$ matrix $\boldsymbol{L}$ that satisfies the detailed balance $L_{mn}f_{eq}(n) = L_{nm}f_{eq}(m)$. One can exploit this property and reformulate the problem in terms of a symmetric matrix $\boldsymbol{K}$ with elements $K_{ij} = \sqrt{L_{ij}L_{ji}}$. Equation 2.17 can then be rewritten as

$$\hat{q}(w|s) = \sqrt{\boldsymbol{f}_{eq}^{T}}(s\boldsymbol{I} - \boldsymbol{K} + iw\boldsymbol{A})^{-1}\sqrt{\boldsymbol{f}_{eq}} \tag{A1}$$

The matrix $\boldsymbol{K}$ can be diagonalized as

$$\boldsymbol{V}^{T}\boldsymbol{K}\boldsymbol{V} = -\boldsymbol{\mu} \qquad \boldsymbol{V}^{T}\boldsymbol{V} = \boldsymbol{I} \tag{A2}$$

where $\boldsymbol{\mu}$ is the diagonal matrix of eigenvalues $\mu_i \geq 0$. The lowest eigenvalue is zero with eigenvector $\sqrt{\boldsymbol{f}_{eq}}$. To minimize the computational effort, our strategy is to first invert the Fourier transform analytically and then the Laplace transform numerically, using the Stehfest algorithm. In practice, the matrix $\boldsymbol{A}$ can be singular; therefore, we rewrite eq A1 as

$$\hat{q}(w|s) = \sqrt{\boldsymbol{f}_{eq}^{T}}\boldsymbol{X}(s)(s\boldsymbol{I} + iw\boldsymbol{Y}(s))^{-1}\boldsymbol{X}(s)\sqrt{\boldsymbol{f}_{eq}} \tag{A3}$$

where

$$X_{ij}(s) = \sum_{n=1}^{N}\frac{V_{in}V_{jn}}{\sqrt{s+\mu_n}}$$

$$Y_{ij}(s) = \sum_{n,m=1}^{N}\frac{V_{in}(\sum_{l=1}^{N}V_{ln}a_lV_{lm})V_{jm}}{\sqrt{(s+\mu_n)(s+\mu_m)}} \tag{A4}$$

Let $\boldsymbol{U}(s)$ be the orthogonal transformation that diagonalizes $\boldsymbol{Y}(s)$:

$$\boldsymbol{U}^{T}(s)\boldsymbol{Y}(s)\boldsymbol{U}(s) = \boldsymbol{\lambda}(s) \tag{A5}$$

where $\boldsymbol{\lambda}(s)$ is the diagonal matrix of eigenvalues. Then,

$$\hat{q}(w|s) = \sum_{n=1}^{N}g_n^2(s)(1 + iw\lambda_n(s))^{-1} \tag{A6}$$

$$g_n(s) = \sum_{l}\sqrt{f_{eq}(l)}[\boldsymbol{X}(s)\boldsymbol{U}(s)]_{ln} \tag{A7}$$

Inverting the Fourier transform, eq A6, and denoting the resulting function as $\hat{Q}(\bar{\alpha}|s)$, we get

$$\hat{Q}(\bar{\alpha}|s) = \sum_{n=1}^{N}g_n^2(s)\frac{\exp(-\bar{\alpha}/\lambda_n(s))}{|\lambda_n(s)|}\theta(\bar{\alpha}\lambda_n(s)) \tag{A8}$$

where $\bar{\alpha} = \bar{a}T$ and $\theta(x)$ is the step function, which is equal to 1 for $x > 0$ and 0 otherwise.

Finally, the Laplace transform, $\hat{Q}(\bar{\alpha}|s)$, is inverted to get $Q(\bar{\alpha}|T)$, which is related to $p(\bar{a}|T)$ by the equation $p(\bar{a}|T) = TQ(\bar{a}T|T)$. For numerical inversion, we use the Stehfest algorithm[14] and find

$$p(\bar{a}|T) = \ln 2 \sum_{j=1}^{2J} C_j \hat{Q}(\bar{a}T|j \ln 2/T) \tag{A9}$$

with coefficients

$$C_j = \sum_{k=[(j+1)/2]}^{\mathrm{Min}(j,J)} \frac{(-1)^{j+J} k^{J+1} (2k)!}{(J-k)!(j-k)!(2k-j)!(k!)^2} \tag{A10}$$

To obtain $p(\bar{a}|T)$ as a function of $\bar{a}$ for fixed T, $2J + 1$ diagonalization of $N \times N$ matrixes is required. In our calculations, we used $J = 8$.

The Stehfest algorithm does not work well for sharp functions. At long times, the distribution does become sharp, but we know the result analytically. A more serious problem arises when $a(r)$ is bounded, i.e., $0 < a(r) < a_M$. In this case, $p(\bar{a}|T)$ is only defined in the interval $0 < \bar{a} < a_M$. This implies that

$$Q(\bar{\alpha}|T) = \theta(T - \bar{\alpha}/a_M) Q'(\bar{\alpha}|T - \bar{\alpha}/a_M) \tag{A11}$$

where $Q'(\bar{\alpha}|T - \bar{\alpha}/a_M)$ is a smooth function of time. In Laplace space, $\hat{Q}'(\bar{\alpha}|s) = \hat{Q}(\bar{\alpha}|s) e^{s\bar{\alpha}/a_M}$. We numerically invert this relation to find $Q'(\bar{\alpha}|T - \bar{\alpha}/a_M)$ and then find $Q(\bar{\alpha}|T)$ in the time domain, using eq A11. As a result, the distribution is calculated for $0 < \bar{a} < a_M$ as

$$p(\bar{a}|T) = \eta \ln 2 \sum_{j=1}^{2J} C_j \hat{Q}(\bar{a}T|j\eta \ln 2/T) e^{j\eta\bar{a} \ln 2/a_m} \tag{A12}$$

where $\eta = (1 - \bar{a}/a_M)^{-1}$ and $\hat{Q}(\bar{\alpha}|s)$ is given by eq A8.

References and Notes

(1) Talaga, D. S.; Lau, W. L.; Roder, H.; Tang, J. Y.; Jia, Y. W.; DeGrado, W. F.; Hochstrasser, R. M. *Proc. Natl. Acad. Sci. U.S.A.* **2000**, *97*, 13021−13026.

(2) Deniz, A. A.; Laurence, T. A.; Beligere, G. S.; Dahan, M.; Martin, A. B.; Chemla, D. S.; Dawson, P. E.; Schultz, P. G.; Weiss, S. *Proc. Natl. Acad. Sci. U.S.A.* **2000**, *97*, 5179−5184.

(3) Schuler, B.; Lipman, E.; Eaton, W. A. *Nature* **2002**, *419*, 743−747.

(4) Carrion-Vazquez, M.; Oberhauser, A. F.; Fowler, S. B.; Marszalek, P. E.; Broedel, S. E.; Clarke, J.; Fernandez, J. M. *Proc. Natl. Acad. Sci. U.S.A.* **1999**, *96*, 3694−3699.

(5) Hummer, G.; Szabo, A. *Proc. Natl. Acad. Sci. U.S.A.* **2001**, *98*, 3658−3661.

(6) Allen, M. P.; Tildesley, D. J. *Computer Simulation of Liquids*; Oxford University Press: New York, 1987.

(7) Geva, E.; Skinner, J. L. *Chem. Phys. Lett.* **1998**, *288*, 225−229.

(8) Berezhkovskii, A. M.; Szabo, A.; Weiss, G. H. *J. Chem. Phys.* **1999**, *110*, 9145−9150.

(9) Uhlenbeck, G. E.; Ornstein, L. S. *Phys. Rev.* **1930**, *36*, 823.

(10) Kubo, R. *J. Phys. Soc. Jpn.* **1954**, *9*, 935.

(11) Anderson, P. W. *J. Phys. Soc. Jpn.* **1954**, *9*, 316.

(12) Kubo, R. In *Fluctuation, Relaxation and Resonance in Magnetic Systems*; ter Haar, D., Ed.; Oliver and Boyd: Edinburgh, U.K., 1962.

(13) Schuss, Z. *Theory and Applications of Stochastic Differential Equations*; Wiley: New York, 1980.

(14) Stehfest, H. *Commun. ACM* **1970**, *13*, 47−48.

(15) Szabo, A.; Schulten, K.; Schulten, Z. *J. Chem. Phys.* **1980**, *72*, 4350−4357.

(16) Socci, N. D.; Onuchic, J. N.; Wolynes, P. G. *J. Chem. Phys.* **1996**, *104*, 5860−5868.

(17) Onuchic, J. N.; Luthey-Schulten, Z.; Wolynes, P. G. *Annu. Rev. Phys. Chem.* **1997**, *48*, 545−600.

(18) Shea, J.-E.; Brooks, C. L., III. *Annu. Rev. Phys. Chem.* **2001**, *52*, 499−535.